

Stromal mesenteric lymph node cells are essential for the generation of gut-homing T cells in vivo

Swantje I. Hammerschmidt,¹ Manuela Ahrendt,² Ulrike Bode,² Benjamin Wahl,¹ Elisabeth Kremmer,³ Reinhold Förster,¹ and Oliver Pabst¹

¹Institute of Immunology and ²Institute of Anatomy, Hannover Medical School, 30625 Hannover, Germany

³Institute of Molecular Immunology, National Research Center for Environment and Health, 81377 Munich, Germany

T cells primed in the gut-draining mesenteric lymph nodes (mLN) are imprinted to express $\alpha 4\beta 7$ -integrin and chemokine receptor CCR9, thereby enabling lymphocytes to migrate to the small intestine. In vitro activation by intestinal dendritic cells (DC) or addition of retinoic acid (RA) is sufficient to instruct expression of these gut-homing molecules. We report that in vivo stroma cells, but not DC, allow the mLN to induce the generation of gut tropism. Peripheral LN (pLN) transplanted into the gut mesenteries fail to support the generation of gut-homing T cells, even though gut-derived DC enter the transplants and prime T cells. DC that fail to induce $\alpha 4\beta 7$ -integrin and CCR9 in vitro readily induce these factors in vivo upon injection into mLN afferent lymphatics. Moreover, uniquely mesenteric but not pLN stroma cells express high levels of RA-producing enzymes and support induction of CCR9 on activated T cells in vitro. These results demonstrate a hitherto unrecognized contribution of stromal cell delivered signals, including RA, on the imprinting of tissue tropism in vivo.

CORRESPONDENCE

Oliver Pabst:
Pabst.Oliver@MH-Hannover.de

Seminal observations demonstrated that lymphocytes isolated from gut-associated lymphoid tissues (GALT) preferentially home to mucosal tissues, whereas lymphocytes isolated from skin-draining LN are biased to enter cutaneous sites (1, 2). Since then the molecular mechanisms underlying these divergent homing properties have been studied in exquisite detail (for a recent review see reference 3). The migration of antigen-experienced T cells into the intestine requires $\alpha 4\beta 7$ -integrin and the chemokine receptor CCR9. $\alpha 4\beta 7$ -Integrin interacts with mucosal vascular addressin cell adhesion molecule 1, which is uniformly expressed by intestinal venules, and $\beta 7$ -integrin-deficient cells are impaired in entering the intestine (4, 5). Expression of the CCR9 ligand CCL25 builds up a gradient with highest expression in the proximal small intestine, low expression in the ileum, and no detectable expression in the colon (6). Consistently, homing of T cells into the proximal small intestine more stringently depends on CCL25-CCR9 interaction compared

with homing into the ileum (7). In contrast, the migration of effector T cells into the skin requires expression of E- and P-selectin ligand and the chemokine receptor CCR4, which endow T cells to interact with the respective ligands expressed in the skin (8). Thus the anatomical site of T cell activation and expansion determines the array of homing factors, including chemokine receptors and integrins, expressed by antigen-experienced T cells. The particular combination of these homing factors specifically targets antigen-experienced T cells to different lymphoid and extralymphoid tissues expressing the respective ligands.

Numerous studies indicated that DC play a decisive role in the imprinting of tissue tropism. In vitro stimulation by GALT-derived DC is sufficient to induce expression of $\alpha 4\beta 7$ -integrin and CCR9 on T cells (9, 10), whereas DC isolated from skin-draining LN confer expression

The online version of this article contains supplemental material.

© 2008 Hammerschmidt et al. This article is distributed under the terms of an Attribution-Noncommercial-Share Alike-No Mirror Sites license for the first six months after the publication date (see <http://www.jem.org/misc/terms.shtml>). After six months it is available under a Creative Commons License (Attribution-Noncommercial-Share Alike 3.0 Unported license, as described at <http://creativecommons.org/licenses/by-nc-sa/3.0/>).

of CCR4 and enzymes required for E- and P-selectin ligand synthesis (11, 12). Such differential function of GALT and peripheral LN (pLN) DC has recently been suggested to reflect their differential ability to produce the vitamin A metabolite retinoic acid (RA). RA is sufficient to direct expression of $\alpha 4\beta 7$ -integrin and CCR9 in vitro irrespective of the origin of the antigen-presenting DC (13). Moreover, addition of RA antagonists impairs up-regulation of gut-homing factors after priming by GALT DC (13). Thus, availability of RA supports the generation of gut-homing T cells, and GALT DC can act as a source for RA in vitro. However, at present the in vivo function of DC-delivered signals in imprinting gut-homing remains speculative. In this paper, we use LN transplantations and DC injection into mesenteric LN (mLN) afferent lymphatics to reveal a hitherto unrecognized essential role of stroma cell-derived signals, including RA, on the generation of tissue tropism in vivo.

RESULTS AND DISCUSSION

mLN but not pLN stroma cells support the generation of gut-homing T cells in vivo

To study the role of LN stroma cells in the generation of gut-homing effector T cells, mLN were excised from WT mice and replaced by either pLN or mLN fragments isolated from EGFP mice. 8 wk after surgery, transplanted LN (Tx-LN) could be identified by their EGFP expression (Fig. 1, A and B). In line with previous observations, we noted that Tx-LN displayed normal tissue architecture and cellular composition (Fig. S1, available at <http://www.jem.org/cgi/content/full/jem.20080039/DC1>) (14) and were connected to gut-draining afferent and LN efferent lymphatics (not depicted) (15). Fluorescent microscopy on T cell zones in Tx-LN revealed that EGFP expression colocalized with gp38 (Fig. 1 C) and ER-TR7 (Fig. 1 D), which are both expressed by LN stroma cells, whereas EGFP⁺ cells showed no overlap with anti-B220 and anti-CD3 staining (not depicted). Similar results were obtained when cells isolated by collagenase digestion of Tx-LN were analyzed by flow cytometry. Few B and T cells, as well as DC, expressed EGFP (Fig. 1 E). Flow cytometry of CD45⁻gp38⁺ stroma cells revealed almost 50% EGFP⁻ cells (Fig. 1 E). Because immunohistology showed that in the T cell zones of Tx-LN the vast majority of stroma cells expressed EGFP, this indicates that donor- and host-derived stroma cells are unevenly distributed in the various compartments of the transplant. In conclusion, a major population of donor-derived nonhematopoietic stroma cells survived in the Tx-LN, whereas the vast majority of hematopoietic cells were constituted by host cells.

To investigate the type of tissue tropism generated in such chimeric Tx-LN, TCR transgenic OT-I or OT-II T cells were fluorescently labeled with CFSE and adoptively transferred into nonmanipulated or transplanted recipients. The frequency of adoptively transferred cells homing into Tx-LN was comparable to endogenous mLN (unpublished data), indicating that Tx-LN were properly vascularized and equipped with the molecular machinery enabling efficient lymphocyte

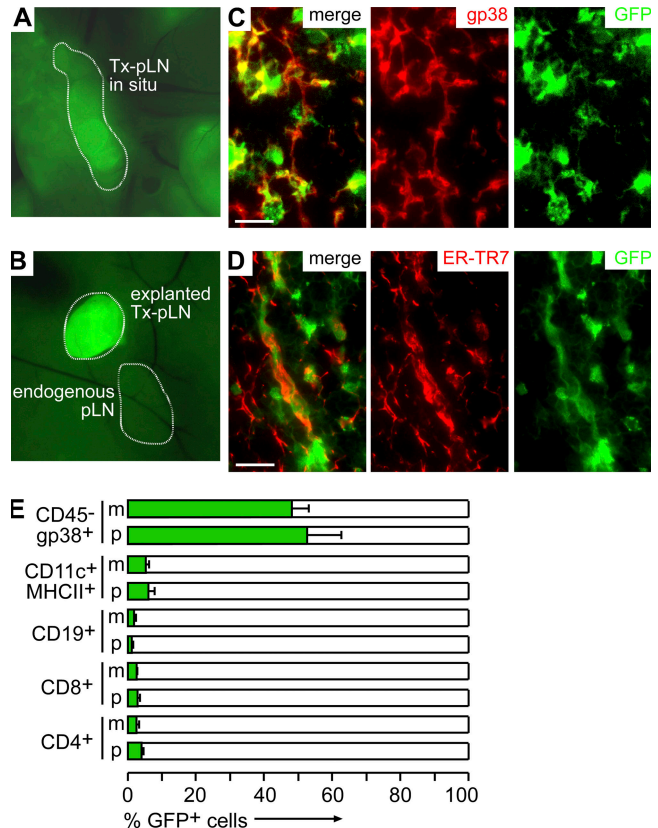


Figure 1. Transplantation of LN fragments yields chimeric LN constituted by donor-derived stromal cells and recipient-derived hematopoietic cells. (A) 8 wk after transplantation, Tx-pLN and Tx-mLN could be identified in situ by expression of EGFP. (B) To demonstrate low autofluorescence in endogenous LN, an excised Tx-pLN was placed beside the endogenous pLN. (C and D) Tx-pLN were analyzed by fluorescence microscopy for EGFP expression (green). Expression of gp38 (C) and ER-TR7 (D) is depicted in red. Comparable results were obtained for Tx-mLN (not depicted). Bars, 20 μ m. (E) Cells were isolated from Tx-LN, and EGFP expression by stroma cells, DC, B, and T cells was analyzed by flow cytometry (data are pooled from four mice analyzed in two experiments). Error bars represent SD.

entry. On the subsequent day, mice were fed with a single dose of Ova, and a group of nontransplanted mice received a single s.c. injection of Ova. 3 d after antigen delivery, cells were isolated from gut-draining endogenous mLN or Tx-LN as well as endogenous skin-draining pLN and analyzed by flow cytometry. In line with previous reports, we observed that in nontransplanted WT mice, feeding of Ova induced T cell proliferation preferentially in the gut-draining mLN but not pLN (16). Expectedly, OT-I T cells proliferating in the endogenous mLN acquired a gut-homing phenotype, characterized by up-regulation of $\alpha 4\beta 7$ -integrin and CCR9 (Fig. 2, A and B). Expression of $\alpha 4\beta 7$ -integrin gradually increased with progressing cell divisions, whereas CCR9 was highly expressed already after one or two rounds of cell division (Fig. 2 B). Similarly, OT-II T cells up-regulated $\alpha 4\beta 7$ -integrin and CCR9 expression in the mLN after antigen

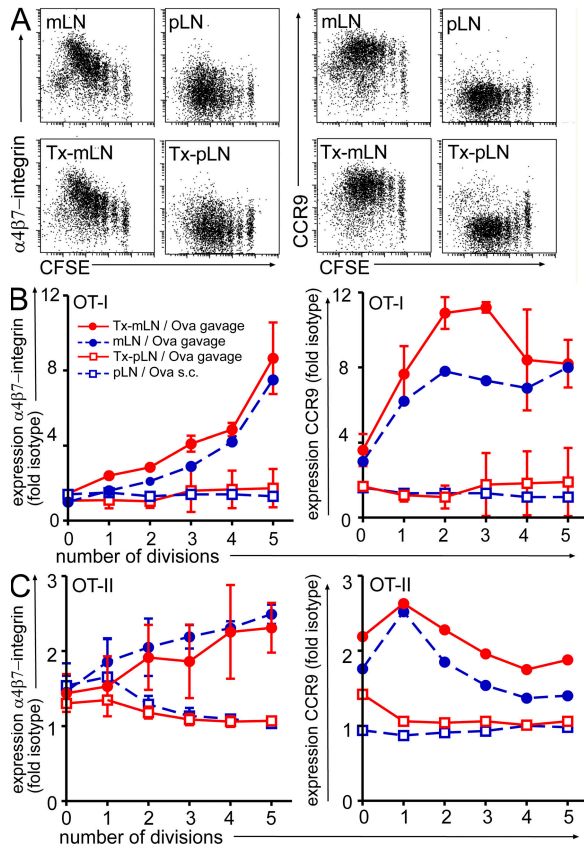


Figure 2. Heterotopic chimeric Tx-pLN, but not orthotopic Tx-mLN, fail to generate gut-homing T cells in vivo. Cells isolated from OT-I or OT-II Ly5.1 mice were labeled with CFSE and adoptively transferred into mice that received Tx-pLN or Tx-mLN 8 wk before. 1 d later, a single dose of Ova was applied orally or injected s.c. (A) Representative results obtained for $\alpha 4\beta 7$ -integrin and CCR9 expression by OT-I T cells (DAPI $^{-}$ V $\alpha 2^{+}$ V $\beta 5^{+}$ CD8 $^{+}$) activated in the mLN, Tx-mLN, and Tx-pLN after oral antigen application and in pLN after s.c. injection of antigen. (B and C) Diagrams depict expression of $\alpha 4\beta 7$ -integrin and CCR9 as fold isotype control for OT-I T cells (DAPI $^{-}$ V $\alpha 2^{+}$ V $\beta 5^{+}$ CD8 $^{+}$; B) and OT-II T cells (DAPI $^{-}$ Ly5.1 $^{+}$ V $\beta 5^{+}$ CD4 $^{+}$; C). All experiments have been performed at least three times with two or more mice per group. Error bars represent SD.

feeding (Fig. 2 C), even though expression levels were lower compared with OT-I T cells. s.c. antigen delivery preferentially resulted in T cell proliferation in the draining inguinal LN, accompanied by no apparent expression of $\alpha 4\beta 7$ -integrin and CCR9 (Fig. 2, A and B).

Comparison of these results obtained from the endogenous LN with the Tx-pLN revealed striking differences: T cells primed in Tx-pLN failed to up-regulate $\alpha 4\beta 7$ -integrin and CCR9. In contrast, grafted Tx-mLN were indistinguishable from endogenous mLN with respect to their ability to promote the generation of gut-homing T cells (Fig. 2, A–C). Notably, oral administration of Ova readily induced proliferation of T cells in Tx-pLN and Tx-mLN comparable to endogenous mLN (Fig. 2 A). Expanding T cells down-regulated CD62L and up-regulated CD44 in Tx-pLN and Tx-mLN to a similar extent, which is indicative of their effector

status (Fig. S2, available at <http://www.jem.org/cgi/content/full/jem.20080039/DC1>). However, because their small size, neither Tx-pLN nor Tx-mLN were able to direct normal numbers of primed OT-I T cells into the small intestine.

Because the induction of T cell proliferation after oral antigen application depends on DC-bound antigen transport (16, 17), the efficient induction of T cell proliferation indicates that gut-derived DC readily entered Tx-LN. Consistently, we observed that compared with endogenous pLN, Tx-pLN contained increased frequencies of DC expressing CD103 $^{+}$, which is indicative of their origin in the small intestinal lamina propria (Fig. S3 A, available at <http://www.jem.org/cgi/content/full/jem.20080039/DC1>). Moreover, orally applied latex beads appeared in Tx-mLN as well as Tx-pLN (Fig. S3 B), a process which requires the active cell-bound transport of the beads. Thus, even though gut-derived DC initiated T cell priming in Tx-pLN and Tx-mLN, divergent homing molecules were induced on the expanding T cells. In particular, gut-derived DC that effectively induce a gut-homing phenotype in vitro are insufficient to sustain the generation of a gut tropism in Tx-pLN in vivo. This suggests that in Tx-LN, donor-derived factors, which are retained after transplantation, essentially shape the type of tissue tropism generated.

Notably, flow cytometry revealed a significant fraction of EGFP $^{-}$ host-derived stroma cells in Tx-LN (Fig. 1 E). Thus we cannot rule out that EGFP $^{-}$ host-derived stroma cells might have seeded the Tx-LN. Transplantation of LN fragments requires puncturing and tearing of the LN capsule before insertion into the mesentery to allow for proper engraftment and vascularization of the transplants. Thus, rebuilding of the capsule and ingrowth of the vasculature most likely will involve substantial contribution of EGFP $^{-}$ host cells. However, apparently these cells are not able to overcome the dominant effect of EGFP $^{+}$ donor-derived stroma on the type of tissue tropism generated in Tx-LN. Moreover, immunohistology showed that in the T cell zones, i.e., at the site of T cell priming, indeed the vast majority of gp38 $^{+}$ stroma cells is donor-derived. We therefore suggest that nonhematopoietic stromal elements are essential for the generation of gut-homing T cells in gut-draining mLN and that these stromal elements differ between pLN and mLN, thereby providing a structural basis for the divergent generation of tissue tropism observed in these LN in vivo.

BM-DC and spleen-derived DC induce gut-homing T cells in vivo but not in vitro

Analyzing the potential of distinct DC subsets to generate gut-homing T cells in vivo requires uncoupling the origin of the DC from their usual destination, i.e., the draining LN. To this aim, we established a new method to inject DC directly into the mLN afferent lymphatics (intralymphatic [i.l.] injection). After oil feeding, the small intestine was exposed by surgery and the mLN afferent lymphatics were located. 10 5 BM-DC was injected into two separate lymphatic vessels opening into the distal aspect of the mLN chain using a fine glass capillary (Fig. 3, A and B). Injection of Ova-loaded

BM-DC readily induced proliferation of only antigen-specific adoptively transferred T cells, indicating that no overt un-specific T cell proliferation was induced. Moreover, DC defective in antigen presentation in the context of either MHC class I or class II failed to provoke T cell proliferation (Fig. 3 C). Thus, T cell proliferation upon i.l. injection of BM-DC reflects the direct priming by the injected DC and does not result from antigen passed on to LN resident DC.

We next explored the phenotype of T cells primed in the mLN upon i.l. injection of DC. As described in the previous paragraph, antigen-loaded DC were injected into mLN afferent lymphatics of WT recipients that previously received CFSE-labeled Ova-specific DO11.10 cells. 3 d later, cells were isolated from the mLN and analyzed for the expression of $\alpha 4\beta 7$ -integrin, CCR9, and E- and P-selectin ligand. For comparison, another group of mice received 10^6 DC-injected s.c., and cells isolated from the skin-draining pLN were analyzed. Strikingly, BM-DC that fail to induce CCR9 on T cells in vitro (Fig. 4 B) (9) efficiently induced CCR9 after i.l. injection in vivo (Fig. 4, A and B). Similarly, in vitro expression of $\alpha 4\beta 7$ -integrin is induced by BM-DC only after prolonged culture (18; for review see reference 3) but was rapidly induced in vivo (Fig. 4, A and B). Thus, T cells primed

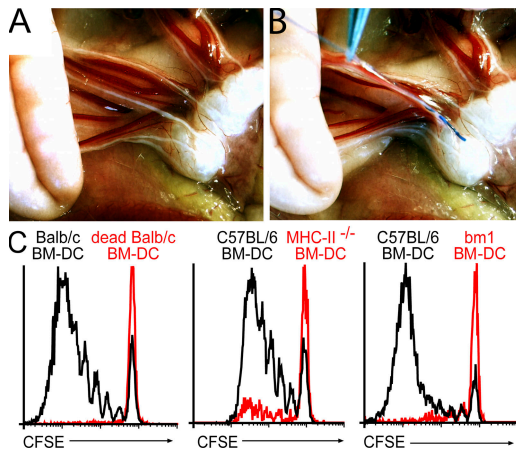


Figure 3. Injection of antigen-loaded BM-DC into mLN afferent lymphatics induces proliferation of antigen-specific T cells. Recipient mice received CFSE-labeled LN cells isolated from DO11.10, OT-I, or OT-II donors. 1 d later, these mice received oil by gavage 1 h before surgery to visualize mLN afferent lymphatics and to facilitate i.l. injection. (A) The small intestine was exposed by surgery and mLN afferent lymphatics were identified by their white color. (B) To demonstrate the method of i.l. injection, $\sim 0.3 \mu\text{l}$ of blue dye was injected into a single lymph vessel. After injection of $2 \times 1 \mu\text{l}$ into two separate vessels, as performed for routine injection of DC, the fluid spread throughout the LN sinus (not depicted). (C) 10^5 BM-DC was injected into two separate lymphatic vessels opening into the distal aspect of the mLN chain. Injection of Ova loaded DC (solid black line), but not heat-killed DC (red line), induced proliferation of Ova-specific DO11.10 T cells (DAPI⁻KJ16-26⁺CD4⁺). BM-DC derived from MHC class II-deficient mice induced only marginal proliferation of OT-II cells. Similarly, DC derived from BM of bm-1 mice failed to activate OT-I T cells. All experiments have been performed at least two times with three or more mice per group.

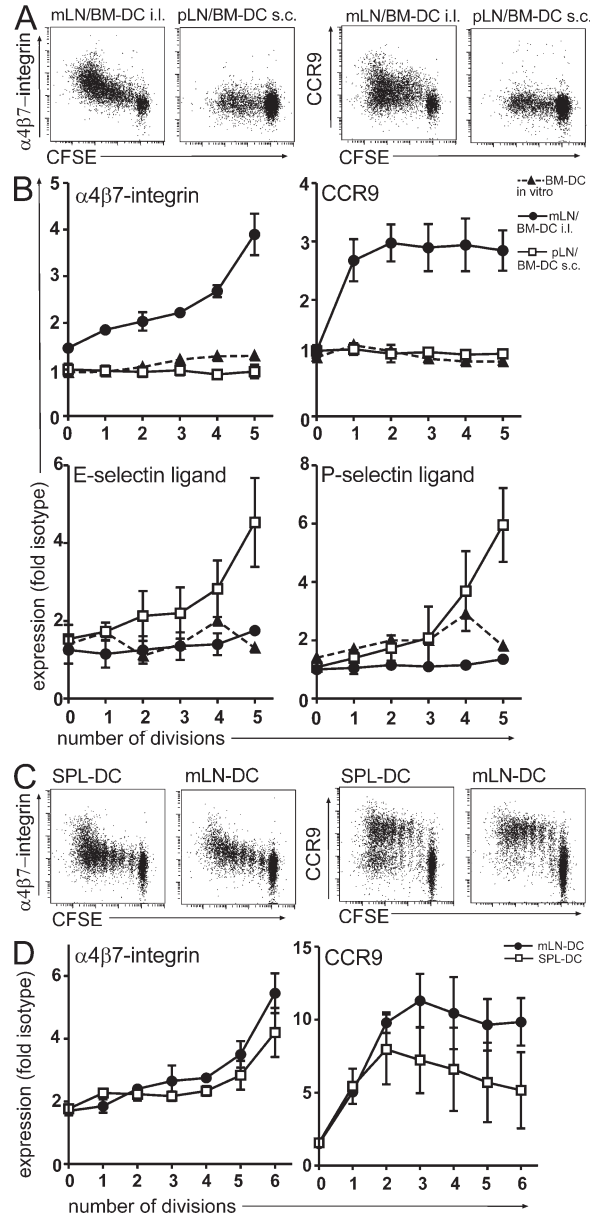


Figure 4. BM-DC and spleen-derived DC generate gut-homing T cells in vivo but not in vitro. (A and B) DO11.10 cells were adoptively transferred into WT recipients. 1 d later, BM-DC were either injected i.l. or s.c., and proliferating DO11.10 T cells in the mLN and pLN were analyzed for expression of $\alpha 4\beta 7$ -integrin, CCR9, and E- and P-selectin ligand as indicated. Moreover, expression of these molecules was assessed after in vitro coculture of antigen-loaded BM-DC with DO11.10 T cells at a 1:10 ratio. BM-DC injected into mLN afferent lymphatics, but not injected s.c., or in vitro cocultures led to the up-regulation of $\alpha 4\beta 7$ -integrin and CCR9 on proliferating T cells. Conversely, s.c., but not i.l., injection of BM-DC induced expression of E- and P-selectin ligand. (C and D) DC were isolated from mLN and spleen, loaded in vitro with Ova peptide, and injected i.l. into recipient mice as described in Fig. 3. Spleen-derived DC that fail to up-regulate gut-homing factors after 3 d of coculture with DO11.10 cells in vitro (not depicted) readily induced expression of $\alpha 4\beta 7$ -integrin and modest expression of CCR9 after i.l. injection in vivo. All experiments were performed at least three times with at least two mice per group.

by BM-DC in vitro largely differ with respect to their homing properties from T cells primed by BM-DC in vivo. We next extended our experiments to primary DC. DC were isolated from spleen or mLN of WT mice and loaded with Ova peptide in vitro. Expectedly, only mLN-derived DC induced a gut-homing phenotype on T cells in vitro (unpublished data). In contrast, both mLN- and spleen-derived DC induced considerable up-regulation of CCR9 and $\alpha 4\beta 7$ -integrin upon i.l. injection (Fig. 4, C and D). In line with these observations, i.p. injection of BM-DC has also been reported to induce expression of $\alpha 4\beta 7$ -integrin on antigen-specific proliferating T cells in the mLN (18). This indicates that even though mLN-derived DC might be more efficient in inducing CCR9 (Fig. 4, C and D) compared with spleen-derived DC, the LN environment and not the origin of DC determines the generation of gut-homing T cells in vivo.

Stroma cells in mLN express RALDH and support the induction of CCR9 in vitro

Because RA can mimic the effects of GALT DC in vitro and addition of RA antagonists counteracts the ability of GALT DC to generate gut-homing T cells, it is tempting to speculate that stroma cells might directly or indirectly influence RA levels in LN. To determine a potential contribution of stromal cells to RA production, we compared the expression of the RA producing enzymes RALDH1, 2, and 3 in purified stroma cells and CD103⁺ and CD103⁻ DC isolated from mLN or pLN. Stroma cells were sorted as CD45⁻CD24⁻gp38⁺ cells to >95% purity and contained no detectable DC (unpublished data). As published previously, RALDH2 expression was substantially higher in CD103⁺ mLN DC compared with their CD103⁻ counterparts (Fig. 5 A) (19). Surprisingly, CD103⁻ pLN DC showed elevated expression levels of RALDH2. This indicates that RALDH2 expression by DC does not necessarily correlate with expression of CD103 or with their ability to instruct CCR9 expression on activated T cells. Interestingly, comparison of RALDH expression between pLN- and mLN-derived stroma cells revealed striking differences. Exclusively mLN-derived stroma cells showed robust expression of RALDH2, whereas expression of this enzyme was virtually absent from pLN stroma cells (Fig. 5 A). Moreover, expression of RALDH1 and 3 was substantially higher in mLN- compared with pLN-derived stroma cells (Fig. 5 A). In contrast, no differences were observed in expression of the Vitamin A–metabolizing alcohol dehydrogenases ADH1, ADH4, and ADH5 (unpublished data).

Next, we directly assessed the ability of LN stroma to support the generation of gut-homing T cells. Because cell sorting of primary LN cell suspensions did not yield sufficient cells for functional assays, LN were enzymatically digested and the resulting cell suspensions plated. Nonadherent cells were repeatedly removed and after 10 d of culture, a dense monolayer of LN-adherent cells with most cells resembling fibroblasts was obtained. Flow cytometry revealed that the vast majority of all cells in such cultures were CD45⁻ and expressed gp38. In contrast, only a minor population of he-

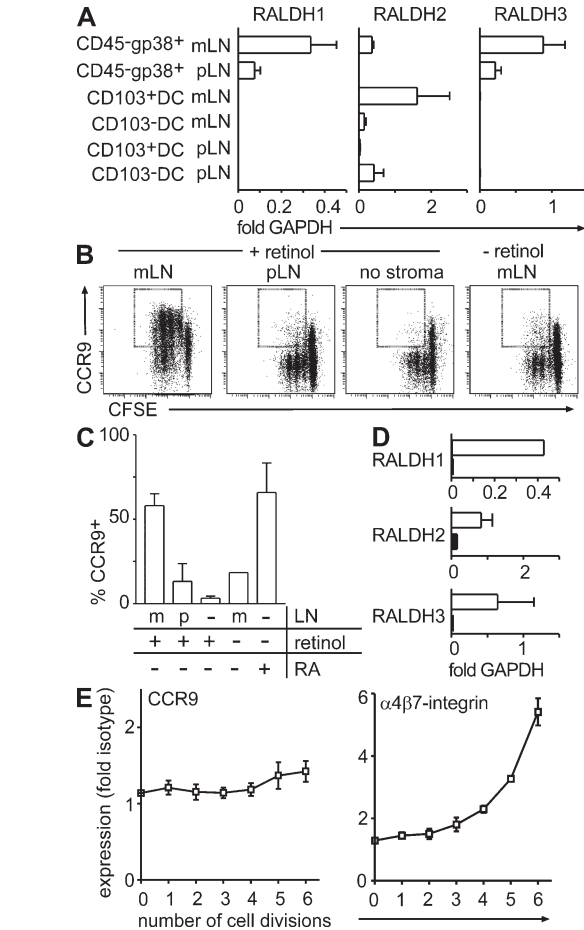


Figure 5. mLN- but not pLN-derived stroma cells express high levels of RALDH and support the induction of CCR9 on proliferating T cells. (A) cDNA was prepared from sorted CD45⁻CD24⁻gp38⁺ stroma cells and CD103⁺ as well as CD103⁻ DC (CD11c⁺MHCII⁺) purified from pLN and mLN. Expression of RALDH1, 2, and 3 was assessed by real-time PCR and is depicted as fold expression compared with GAPDH. Data depict the mean and SD of three to five independent experiments measured in duplicates. (B and C) CFSE-labeled OT-I cells were activated by anti-CD3/CD28 treatment in the presence of either pLN- or mLN-derived stroma cells with or without addition of retinol. Stroma cells were enriched by adherence and culture of digested LN cell suspensions over 10 d. Data shown represent the mean and SD of three independent experiments. (D) cDNA was prepared from sorted CD45⁻CD24⁻gp38⁺ stroma cells (open bars) and CD103⁺ DC (closed bars) of CCR7-deficient mLN. Expression of RALDH1, 2, and 3 was assessed by real-time PCR. Bars depict the mean and SD of fold expression compared with GAPDH observed in two independent experiments. (E) CCR9 expression was analyzed after i.l. injection of antigen-loaded BM-DC into mLN afferent lymphatics of CCR7-deficient mice. In contrast to the situation in WT mice, BM-DC failed to support the induction of CCR9 on T cells in CCR7-deficient mice. Expression of $\alpha 4\beta 7$ -integrin was not significantly affected. Results depict data obtained in one out of two experiments performed with five mice. Error bars represent SD.

matopoietic cells was observed ($2.4 \pm 2.2\%$ of all cells expressed CD11b and $1.5 \pm 1.4\%$ of cells coexpressed CD11c and MHCII; $n = 7$) and real-time PCR assays did not show

any expression of MHCII. Thus, we suggest that such cultures of LN-adherent cells do not contain functionally relevant populations of DC or macrophages and can be used as a substitute for primary isolates of LN stroma cells. Interestingly, OT-I T cells activated by anti-CD3/CD28 stimulation readily up-regulated expression of CCR9 in the presence of adherent cells cultured out of mLN but not pLN (Fig. 5, B and C). Up-regulation of CCR9 was dependent on the presence of retinol, suggesting that the ability of mLN but not pLN stroma-adherent cells to metabolize retinol was responsible for the induction of CCR9 (Fig. 5, B and C). We therefore suggest that the particular ability of mLN to support the generation of gut-homing T cells, at least in part, relies on the ability of mLN stroma cells to produce RA.

RA is well known to act as a signaling molecule eliciting RA-dependent responses throughout tissues, as exemplified by the rescue of morphogenetic defects in RALDH2-deficient embryos by low chimerism with WT cells (20). Moreover, RA can enhance its own production by up-regulation of the enzymatic machinery regulating RA levels. Thus the combined function of LN-resident stroma cells and migrating DC, both of which express high levels of RALDH genes, might integrate to shape the unique properties of LN, including the particular ability of mLN to direct effector T cells into the gut.

In line with this idea, we observed that BM-DC failed to induce expression of CCR9 upon i.l. injection in the mLN of CCR7-deficient mice (Fig. 5 E). CCR7-deficient mice are characterized by impaired steady-state migration of DC, have a strongly reduced population of CD103⁺ DC in their mLN (16, 21), and residual CD103⁺ DC in the mLN of CCR7-deficient mice almost completely lack expression of RALDH2 (Fig. 5 D). Up-regulation of α 4 β 7-integrin, as well as expression of RALDH genes by mLN stroma cells, was not significantly altered in CCR7-deficient mice (Fig. 5, D and E). Therefore, in vivo, the generation of gut tropism, i.e., expression of CCR9, appears to require instructive signals by both mLN resident stroma cells and DC. These signals are likely to include the agonistic effects of RA on the induction of CCR9 and α 4 β 7-integrin and appear to influence proliferating T cells in trans. In contrast, RA provided in cis by the antigen-presenting DC appears to play a subordinate role, as revealed by the ability of RALDH2-negative spleen DC to induce CCR9 after i.l. injection and the inability of Tx-pLN to support the induction of gut tropic T cells. Still, RA provided in cis by the antigen-presenting DC might add to the net regulation of tissue tropic factors, as reflected by the more potent activity of mLN-derived DC to induce CCR9 compared with spleen-derived DC after i.l. injection.

Recently, an additional role for RA has been reported in the generation of regulatory T cells (19, 22–24). Interestingly, conversion of naive T cells into regulatory T cells occurs more efficiently in GALT than other tissues (19, 23), raising the possibility that regulation of RA levels by LN stroma cells does not only affect tissue tropisms but, more-

over, might influence the balance between effector and regulatory T cell generation.

In conclusion, we suggest that in vivo, gut-homing T cells can only be generated in a permissive LN environment that is determined by resident stroma cells and DC. Resident stroma cells might produce negative signals that impair the generation of gut-homing T cells in Tx-pLN. Additionally, mLN stroma cells deliver positive signals, including RA, that support the induction of α 4 β 7-integrin and CCR9 on T cells by DC that fail to promote this process in vitro. Under physiological conditions, stroma cells and DC might cooperate in shaping a LN environment that in the mLN is distinguished by high levels of RA, favoring the induction of gut-homing molecules. This balance is perturbed by LN transplantation and i.l. injection, revealing the major influence of stromal cells in LN function.

MATERIALS AND METHODS

Mouse strains. C57BL/6, C57BL/6-Tg(Tcra Tcrb)1100Mjbj (designated here as OT-I mice; OT-I T cells selectively recognize Ova peptide presented in the context of MHC class I), C57BL/6-Tg(Tcra Tcrb)425Cbn-Ptprc^a (designated here as OT-II Ly5.1 mice; OT-II T cells selectively recognize Ova peptide presented in the context of MHC class II), B6.C-H2^{bm1} (designated here as bm1-mice; bm-1 mice carry a mutated H2-K molecule and cannot present Ova peptide in the context of MHC class I), B6;129-H2^{dab1} (designated here as MHC class II-deficient mice; mice were provided by G. Behrens, Clinical Immunology and Rheumatology, Hannover Medical School, Hannover, Germany), C57BL/6-Tg(ACTbEGFP) (designated here as EGFP mice; these mice constitutively express EGFP in all cells under the control of the chicken β -actin promoter), BALB/c, and BALB/c-Tg(DO11.10) were bred at the central animal facility of Hannover Medical School under specific pathogen-free conditions. BALB/c mice were purchased from Charles River Laboratories. All experiments have been approved by the institutional review board and the “Niedersächsisches Landesamt für Verbraucherschutz und Lebensmittelsicherheit.”

Antibodies and reagents. The following antibodies, fusion proteins, and conjugates were used in this study: anti-CD11c-APC (HL3), anti-MHCII (1A^b)-bio (AF6-120.1), anti-V β 5.1, 5.2 TCR-bio (MR9-4), anti-V α 2-PE (B20.1), anti- α 4 β 7 (DTAK32), and CD45.2-PerCp-Cy5.5 (104) (BD Biosciences); anti-DO11.10 TCR-bio (KJ1-26) (Caltag Laboratories); ER-TR7 (BMA Biomedicals); and recombinant mouse E-Selectin/Fc chimera and recombinant mouse P-Selectin/Fc chimera (R&D Systems). Anti-CD4 (RmCD4.2), anti-CD3 (17A2), anti-CD8 β (RmCD8-2), anti-B220 (TIB146), anti-CCR9 (7E7), and anti-gp38 (8.1.1) antibodies were produced in our laboratory. Cy3 and Cy5 conjugates (GE Healthcare), as well as Pacific Orange conjugates (Invitrogen), were prepared as recommended by the manufacturer. Biotinylated antibodies were recognized by streptavidin coupled to PerCp (BD Biosciences). Anti-CCR9 and anti- α 4 β 7 were detected using mouse anti-rat Cy5 (Jackson ImmunoResearch Laboratories). E-Selectin/Fc chimera and P-Selectin/Fc chimera were detected with goat anti-human Cy5 (Jackson ImmunoResearch Laboratories).

Intestinal surgery. Under the combined anesthesia with Ketamine and Rompun, mesenteric lymphadenectomy was performed by microdissection along the length of the superior mesenteric artery to aortic root. mLN or pLN (inguinal, axillary, and brachial LN) were isolated from EGFP mice and grafted into the site of the removed mLN. Mice were used for experiments 8 wk after transplantation. Immunohistology of grafted LN was performed as previously described (25).

Adoptive cell transfer. Cells were isolated from DO11.10, OT-II Ly5.1, or OT-I transgenic mice expressing TCR recognizing Ova (Ovalbumin),

labeled with CFSE as described previously (16), and i.v. transferred into syngeneic recipients. Mice received a single dose of 100 mg Ova by gavage. BM-DC were prepared as previously described (26) and loaded with antigen by addition of 1 mg/ml Ova during the maturation. BM-DC were washed thoroughly and injected i.l. or s.c. into adoptively transferred recipients. For s.c. transfers, 10^6 DC were injected into the dorsal flank. Mice receiving DC i.l. were gavaged with 200 μ l of olive oil 1 h before surgery for better visualization of mesenteric lymph vessels. Under the combined anesthesia with Ketamine and Rompun, mLN afferent lymphatics were exposed and 10^5 DC in a volume of $2 \times 1 \mu$ l were injected with a fine glass needle into two separate lymph vessels.

Cell isolation. For isolation of DC, lymphoid organs were digested at 37°C for 45 min with 0.5 mg/ml Collagenase A and 50 U/ml DNase I (both Roche) in RPMI 1640/10% FCS. RBC were lysed and CD11c⁺ cells were enriched by CD11c Microbeads using AutoMACS (Miltenyi Biotec), yielding a mean purity of 70% MHCII⁺CD11⁺ DC. Enriched DC suspensions were pulsed with 1 μ g/ml OVA peptide (323–329) binding to MHC class II for 1 h at 37°C and washed thoroughly before i.l. injection. For isolation of stroma cells, LN were digested at 37°C for 60 min with 0.1 mg/ml Liberase Blendzyme 2 (Roche) and 50 U/ml DNase I. Hematopoietic cells were depleted by anti-CD45 anti-CD11c MACS negative selection and purified by FACS sorting (FACS Aria; BD Biosciences) as DAPI⁻CD45⁻CD24⁻gp38⁺ cells for isolation of RNA. Alternatively, digested LN cell suspensions were cultured in DMEM/10% FCS/PS for 10 d. Medium was exchanged every second day to remove nonadherent cells from the cultures.

In vitro cocultures. 10^5 CFSE-labeled OT-I cells were activated by adding 10^5 antigen-loaded DC. For stroma cell cocultures, 2.5×10^5 CFSE-labeled purified CD8⁺ OT-I cells (CD8⁺ T Cell Isolation kit; Miltenyi Biotec) were activated with CD3/CD28 beads (Invitrogen) in the absence or presence of 50 nM retinol or 5 nM RA (both Sigma-Aldrich).

Real-time PCR. RNA was isolated using the Absolutely RNA Microprep kit (Stratagene) and converted into cDNA (Superscript II reverse transcription; Invitrogen) using random hexamer primers. Expression of GAPDH and RALDH1, 2, and 3 was analyzed using a LightCycler 2.0 (Roche) and SYBR Premix Ex Taq kit (Takara Bio Inc.). The following primers were used: RALDH1 (forward), CTCCTCTCACGGCTCTTCA; RALDH1 (reverse), AATGTTTACCACGCCAGGAG; RALDH2 (forward), CATGGTATCCTCCGCAATG; RALDH2 (reverse), GCGCATTTAAGGCA-TTGTAAC; RALDH3 (forward), AACCTGGACAAAGCACTGAAG; RALDH3 (reverse), AATGCATTGTAGCAGTTGATCC; and GAPDH (forward), TGCACCACCAACTGCTTAG.

Statistical analysis. Statistical analysis was performed with Prism software (GraphPad Software, Inc.). All significant values were determined using the unpaired two-tailed *t* test and error bars represent SD. Statistical differences for the mean values are indicated as follows: *, *P* < 0.05; **, *P* < 0.01; ***, *P* < 0.001.

Online supplemental material. Fig. S1 shows that Tx-LN display normal cellular composition and LN architecture. Fig. S2 shows that proliferating T cells in Tx-LN gain a phenotype indicative for activated T cells. Fig. S3 shows that gut-derived DC enter Tx-LN. Online supplemental material is available at <http://www.jem.org/cgi/content/full/jem.20080039/DC1>.

We thank Georg Behrens for providing MHC class II-deficient-mice and Immo Prinz, Andreas Krueger, and William W. Agace for discussion and comments on the manuscript.

This work was supported by Deutsche Forschungsgemeinschaft grants (SFB621-A1 to R. Förster and SFB621-A11 to O. Pabst).

The authors have no conflicting financial interests.

Submitted: 4 January 2008

Accepted: 17 September 2008

REFERENCES

- McDermott, M.R., and J. Bienenstock. 1979. Evidence for a common mucosal immunologic system. I. Migration of B immunoblasts into intestinal, respiratory, and genital tissues. *J. Immunol.* 122:1892–1898.
- Cahill, R.N., D.C. Poskitt, D.C. Frost, and Z. Trmka. 1977. Two distinct pools of recirculating T lymphocytes: migratory characteristics of nodal and intestinal T lymphocytes. *J. Exp. Med.* 145:420–428.
- Agace, W.W. 2006. Tissue-tropic effector T cells: generation and targeting opportunities. *Nat. Rev. Immunol.* 6:682–692.
- Wagner, N., J. Lohler, E.J. Kunkel, K. Ley, E. Leung, G. Krissansen, K. Rajewsky, and W. Müller. 1996. Critical role for beta7 integrins in formation of the gut-associated lymphoid tissue. *Nature.* 382:366–370.
- Lefrancois, L., C.M. Parker, S. Olson, W. Muller, N. Wagner, M.P. Schon, and L. Puddington. 1999. The role of $\beta 7$ integrins in CD8 T cell trafficking during an antiviral immune response. *J. Exp. Med.* 189:1631–1638.
- Ericsson, A., K. Kotarsky, M. Svensson, M. Sigvardsson, and W. Agace. 2006. Functional characterization of the CCL25 promoter in small intestinal epithelial cells suggests a regulatory role for caudal-related homeobox (Cdx) transcription factors. *J. Immunol.* 176:3642–3651.
- Stenstad, H., M. Svensson, H. Cucak, K. Kotarsky, and W.W. Agace. 2007. Differential homing mechanisms regulate regionalized effector CD8 α beta⁺ T cell accumulation within the small intestine. *Proc. Natl. Acad. Sci. USA.* 104:10122–10127.
- Austrup, F., D. Vestweber, E. Borges, M. Lohning, R. Brauer, U. Herz, H. Renz, R. Hallmann, A. Scheffold, A. Radbruch, and A. Hamann. 1997. P- and E-selectin mediate recruitment of T-helper-1 but not T-helper-2 cells into inflamed tissues. *Nature.* 385:81–83.
- Johansson-Lindbom, B., M. Svensson, M.A. Wurbel, B. Malissen, G. Marquez, and W. Agace. 2003. Selective generation of gut tropic T cells in gut-associated lymphoid tissue (GALT): requirement for GALT dendritic cells and adjuvant. *J. Exp. Med.* 198:963–969.
- Mora, J.R., M.R. Bono, N. Manjunath, W. Weninger, L.L. Cavanagh, M. Roseblatt, and U.H. Von Andrian. 2003. Selective imprinting of gut-homing T cells by Peyer's patch dendritic cells. *Nature.* 424:88–93.
- Mora, J.R., G. Cheng, D. Picarella, M. Briskin, N. Buchanan, and U.H. von Andrian. 2005. Reciprocal and dynamic control of CD8 T cell homing by dendritic cells from skin- and gut-associated lymphoid tissues. *J. Exp. Med.* 201:303–316.
- Dudda, J.C., J.C. Simon, and S. Martin. 2004. Dendritic cell immunization route determines CD8⁺ T cell trafficking to inflamed skin: role for tissue microenvironment and dendritic cells in establishment of T cell-homing subsets. *J. Immunol.* 172:857–863.
- Iwata, M., A. Hirakiyama, Y. Eshima, H. Kagechika, C. Kato, and S.Y. Song. 2004. Retinoic acid imprints gut-homing specificity on T cells. *Immunity.* 21:527–538.
- Wolvers, D.A., C.J. Coenen-de Roo, R.E. Mebius, M.J. van der Cammen, F. Tirion, A.M. Miltenburg, and G. Kraal. 1999. Intranasally induced immunological tolerance is determined by characteristics of the draining lymph nodes: studies with OVA and human cartilage gp-39. *J. Immunol.* 162:1994–1998.
- Ahrendt, M., S. Hammerschmidt, O. Pabst, R. Pabst, and U. Bode. 2008. Stromal cells confer lymph node-specific properties by shaping a unique microenvironment influencing local immune responses. *J. Immunol.* 181:1898–1907.
- Worbs, T., U. Bode, S. Yan, M.W. Hoffmann, G. Hintzen, G. Bernhardt, R. Forster, and O. Pabst. 2006. Oral tolerance originates in the intestinal immune system and relies on antigen carriage by dendritic cells. *J. Exp. Med.* 203:519–527.
- Pabst, O., G. Bernhardt, and R. Forster. 2007. The impact of cell-bound antigen transport on mucosal tolerance induction. *J. Leukoc. Biol.* 82:795–800.
- Dudda, J.C., A. Lembo, E. Bachtanian, J. Huehn, C. Siewert, A. Hamann, E. Kremmer, R. Forster, and S.F. Martin. 2005. Dendritic cells govern induction and reprogramming of polarized tissue-selective homing receptor patterns of T cells: important roles for soluble factors and tissue microenvironments. *Eur. J. Immunol.* 35:1056–1065.

19. Coombes, J.L., K.R. Siddiqui, C.V. Arancibia-Carcamo, J. Hall, C.M. Sun, Y. Belkaid, and F. Powrie. 2007. A functionally specialized population of mucosal CD103⁺ DCs induces Foxp3⁺ regulatory T cells via a TGF- β - and retinoic acid-dependent mechanism. *J. Exp. Med.* 204:1757–1764.
20. Vermot, J., N. Messaddeq, K. Niederreither, A. Dierich, and P. Dolle. 2006. Rescue of morphogenetic defects and of retinoic acid signaling in retinaldehyde dehydrogenase 2 (Raldh2) mouse mutants by chimerism with wild-type cells. *Differentiation*. 74:661–668.
21. Ohl, L., M. Mohaupt, N. Czeloth, G. Hintzen, Z. Kiafard, J. Zwirner, T. Blankenstein, G. Henning, and R. Forster. 2004. CCR7 governs skin dendritic cell migration under inflammatory and steady-state conditions. *Immunity*. 21:279–288.
22. Mucida, D., Y. Park, G. Kim, O. Turovskaya, I. Scott, M. Kronenberg, and H. Cheroutre. 2007. Reciprocal TH17 and regulatory T cell differentiation mediated by retinoic acid. *Science*. 317:256–260.
23. Sun, C.M., J.A. Hall, R.B. Blank, N. Bouladoux, M. Oukka, J.R. Mora, and Y. Belkaid. 2007. Small intestine lamina propria dendritic cells promote de novo generation of Foxp3 T reg cells via retinoic acid. *J. Exp. Med.* 204:1775–1785.
24. Benson, M.J., K. Pino-Lagos, M. Roseblatt, and R.J. Noelle. 2007. All-trans retinoic acid mediates enhanced T reg cell growth, differentiation, and gut homing in the face of high levels of co-stimulation. *J. Exp. Med.* 204:1765–1774.
25. Pabst, O., H. Herbrand, T. Worbs, M. Friedrichsen, S. Yan, M.W. Hoffmann, H. Korner, G. Bernhardt, R. Pabst, and R. Forster. 2005. Cryptopatches and isolated lymphoid follicles: dynamic lymphoid tissues dispensable for the generation of intraepithelial lymphocytes. *Eur. J. Immunol.* 35:98–107.
26. Czeloth, N., G. Bernhardt, F. Hofmann, H. Genth, and R. Forster. 2005. Sphingosine-1-phosphate mediates migration of mature dendritic cells. *J. Immunol.* 175:2960–2967.